

# Functionalization of Two-Dimensional MoS<sub>2</sub>: On the Reaction Between MoS<sub>2</sub> and Organic Thiols

Xin Chen, Nina C. Berner, Claudia Backes, Georg S. Duesberg, and Aidan R. McDonald\*

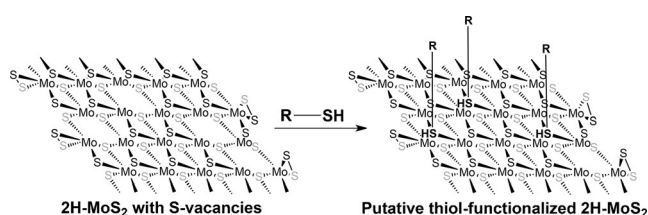
**Abstract:** Two-dimensional layered transition metal dichalcogenides (TMDs) have attracted great interest owing to their unique properties and a wide array of potential applications. However, due to their inert nature, pristine TMDs are very challenging to functionalize. We demonstrate a general route to functionalize exfoliated 2H-MoS<sub>2</sub> with cysteine. Critically, MoS<sub>2</sub> was found to be facilitating the oxidation of the thiol cysteine to the disulfide cystine during functionalization. The resulting cystine was physisorbed on MoS<sub>2</sub> rather than coordinated as a thiol (cysteine) filling S-vacancies in the 2H-MoS<sub>2</sub> surface, as originally conceived. These observations were found to be true for other organic thiols and indeed other TMDs. Our findings suggest that functionalization of two-dimensional MoS<sub>2</sub> using organic thiols may not yield covalently or datively tethered functionalities, rather, in this instance, they yield physisorbed disulfides that are easily removed.

In the rich family of two-dimensional (2D) layered nanomaterials, layered transition metal dichalcogenides (TMDs) have sparked increasing interest owing to their unique structures, wide range of chemical compositions, and a vast array of unique physical properties.<sup>[1–11]</sup> TMDs have potential applications in electronic devices, optoelectronics, sensing, energy storage, and catalysis.<sup>[1–14]</sup> A major focus of experimental research in recent years has concentrated on the development of synthetic routes to produce high-quality TMD nanosheets.<sup>[14–20]</sup> However, routes towards the efficient high-yield synthesis or exfoliation of TMDs remain lacking, hindering the production of large quantities of TMD nanosheets. Functionalization of such layered materials could facilitate the production of higher quantities of 2D TMDs, while also allowing for the tuning of their physical properties.

Molybdenum disulfide (MoS<sub>2</sub>) is a prototypical TMD and acts as an excellent model system to explore the chemistry of 2D TMDs. 2D MoS<sub>2</sub> is most often isolated as one of two

polymorphs:<sup>[14]</sup> in 2H-MoS<sub>2</sub> S-atoms coordinate to the Mo-atom in a trigonal prismatic fashion, whereas in 1T-MoS<sub>2</sub> the Mo-atom is octahedrally ligated. Importantly, thin layered 2H- and 1T-MoS<sub>2</sub> display different properties, 2H-MoS<sub>2</sub> is a semi-conductor (energy gap  $\approx 1.2$  eV) and a photoluminophore,<sup>[21,22]</sup> whereas 1T-MoS<sub>2</sub> is metallic and does not photoluminesce.<sup>[3]</sup> The covalent functionalization of 1T-MoS<sub>2</sub> has recently been reported,<sup>[23,24]</sup> employing a rather harsh chemical exfoliation (ce) procedure. No well-characterized examples of covalent functionalization of 2H-MoS<sub>2</sub> have been reported to date. We recently reported the mild functionalization of 2H-MoS<sub>2</sub> through ligation of surface S-atoms to coordination complexes,<sup>[25]</sup> our efforts are now focused on exploring routes towards the covalent functionalization of 2H-MoS<sub>2</sub>.

Recent reports have claimed the functionalization of both ce-1T- and 2H-MoS<sub>2</sub> by reaction with organic thiols. In a seminal paper, Dravid and co-workers described the reaction between ce-1T-MoS<sub>2</sub> and organic thiols yielding functionalized ce-1T-MoS<sub>2</sub>.<sup>[26]</sup> This was described as “ligand conjugation” to ce-1T-MoS<sub>2</sub>, presumably meaning coordination of the thiol to Mo-atoms at S-vacancies (by forming a dative Mo–S bond). Later work has demonstrated further applications of this technique.<sup>[27–35]</sup> Unfortunately, in all of these reports, there remains little to no insight into the thiol ligand/MoS<sub>2</sub> interaction. At the inception of this work, we too postulated that 2H-MoS<sub>2</sub> could be functionalized using organic thiols by coordination of the thiol group to Mo-atoms at S-atom vacancies (Scheme 1). Herein, we present



**Scheme 1.** Proposed method to functionalize 2D 2H-MoS<sub>2</sub> at sulfur vacancies.

the one-step surface functionalization of 2H-MoS<sub>2</sub> nanosheets with an organic thiol (cysteine), resulting in functionalized 2H-MoS<sub>2</sub>. We explore in detail the thiol/MoS<sub>2</sub> interaction and show that organic thiols may actually be physisorbed on MoS<sub>2</sub> as disulfides, rather than undergoing any bond-forming process with the MoS<sub>2</sub>.

As we reported previously,<sup>[25]</sup> in the functionalization of 2H-MoS<sub>2</sub> it was necessary to disperse few-layer thick 2H-

[\*] X. Chen, Dr. N. C. Berner, Dr. C. Backes, Prof. Dr. G. S. Duesberg, Dr. A. R. McDonald  
CRANN/AMBER Nanoscience Institute  
Trinity College Dublin  
The University of Dublin  
College Green, Dublin 2 (Ireland)  
E-mail: aidan.mcdonald@tcd.ie

X. Chen, Dr. N. C. Berner, Prof. Dr. G. S. Duesberg,  
Dr. A. R. McDonald  
School of Chemistry, Trinity College Dublin  
Dr. C. Backes  
School of Physics, Trinity College Dublin

Supporting information for this article can be found under:  
<http://dx.doi.org/10.1002/anie.201510219>.

MoS<sub>2</sub> in 2-propanol (IPA), and not the standard (toxic) dispersion/exfoliating solvents *N*-methyl-2-pyrrolidone (NMP) or *N*-cyclohexyl-2-pyrrolidone (CHP).<sup>[3,15]</sup> The IPA dispersions of 2H-MoS<sub>2</sub> displayed a mean lateral dimension  $\langle L \rangle$  of  $\approx 260$  nm and degree of exfoliation  $\langle N \rangle$  of 9–10 layers. The IPA-exfoliated 2H-MoS<sub>2</sub> was thus an ideal 2D TMD dispersion for functionalization studies.

2H-MoS<sub>2</sub> normally displays S:Mo ratios of approximately 1.8:1 ( $\pm 0.2$ ), as suggested by X-ray photoelectron spectroscopy (XPS).<sup>[25,36]</sup> Transmission electron microscopy (TEM) analysis corroborated this, showing that basal-plane S-vacancies were common.<sup>[32,37,38]</sup> We postulated that thiol-containing organic molecules could fill these sulfur vacancies (Scheme 1). To test this hypothesis we reacted liquid-exfoliated 2H-MoS<sub>2</sub> with a thiol-containing organic molecule, cysteine. Cysteine was chosen because it is bio-relevant, commercially available, and contains functional groups (carboxylate and amine) that would allow for simple characterization and further derivatization. 2H-MoS<sub>2</sub> nanosheets ( $0.5 \text{ g L}^{-1}$ ) dispersed in IPA (20 mL) were reacted with the hydrochloride salt of L-cysteine dissolved in IPA ( $20 \text{ g L}^{-1}$ , 10 mL) by combining the dispersion and solution and performing tip ultra-sonication on the mixture for 0.5 h at room temperature (Supporting Information). Following the ultra-sonication, the resulting dispersion was subjected to high-speed centrifugation to precipitate all dispersed materials. The resulting sediment was exhaustively washed with aqueous solutions, and then re-dispersed in IPA (10 mL) for further characterization.

The cysteine-functionalized re-dispersed 2H-MoS<sub>2</sub> (Cys-2H-MoS<sub>2</sub>) displayed a markedly different dispersability in IPA compared to pristine 2H-MoS<sub>2</sub>. The electronic extinction spectrum of Cys-2H-MoS<sub>2</sub> displayed a very high degree of nanosheet aggregation, as evidenced by the rather large baseline shift when comparing pristine 2H-MoS<sub>2</sub> to Cys-2H-MoS<sub>2</sub> (Figure 1a).<sup>[39]</sup> This difference was noticeable to the human eye (Figure 1b); Cys-2H-MoS<sub>2</sub> flocculated (formed clumpy materials) readily in IPA, whereas dispersions of pristine 2H-MoS<sub>2</sub> did not. Furthermore, Cys-2H-MoS<sub>2</sub> yielded dispersions that were black in color, whereas pristine 2H-MoS<sub>2</sub> dispersions tended to be yellowish green. These

observations clearly indicate that the surface properties in the Cys-2H-MoS<sub>2</sub> had been altered dramatically compared to pristine 2H-MoS<sub>2</sub>.

Importantly, functionalization appeared to have caused minimal changes to the relative intensities or energies of excitonic transitions attributed to exfoliated 2H-MoS<sub>2</sub> (Figure 1a). The transitions at  $\lambda_{\text{max}} = 459$ , 614, and 675 nm are typical of 2H-MoS<sub>2</sub>. Cys-2H-MoS<sub>2</sub> displayed a similar set of features ( $\lambda_{\text{max}} = 496$ , 629, and 689 nm), displaying a small degree of red-shifting compared to the parent pristine 2H-MoS<sub>2</sub>, which could be caused by the rather large baseline shift caused by flocculation. These observations are very important because they establish that functionalization yielded a slightly modified 2H-MoS<sub>2</sub> and, critically, did not yield the 1T-polytype (1T-MoS<sub>2</sub> has an extinction spectrum very different from 2H-MoS<sub>2</sub>).<sup>[21]</sup> Most other covalent functionalization techniques to date have yielded 1T-MoS<sub>2</sub>.

Comparison of the diffuse reflectance infrared Fourier transform (DRIFT) spectra of 2H-MoS<sub>2</sub> and Cys-2H-MoS<sub>2</sub> demonstrated a sharp feature at  $384 \text{ cm}^{-1}$  that is typical of 2H-MoS<sub>2</sub> (Figure 2),<sup>[40]</sup> indicating that the functionalization had not affected the vibrational properties or overall morphology

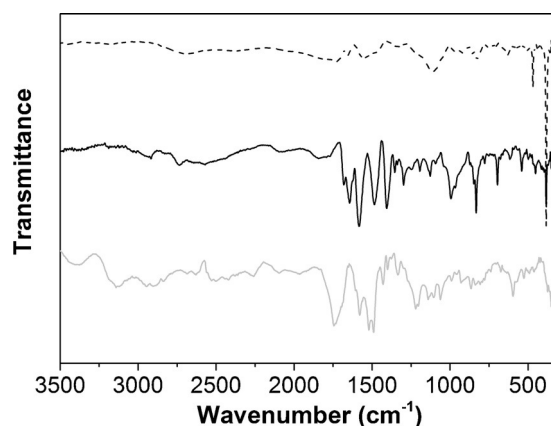


**Figure 2.** DRIFT spectra of pristine 2H-MoS<sub>2</sub> (dashed trace), Cys-2H-MoS<sub>2</sub> (solid trace) and cysteine (gray trace).

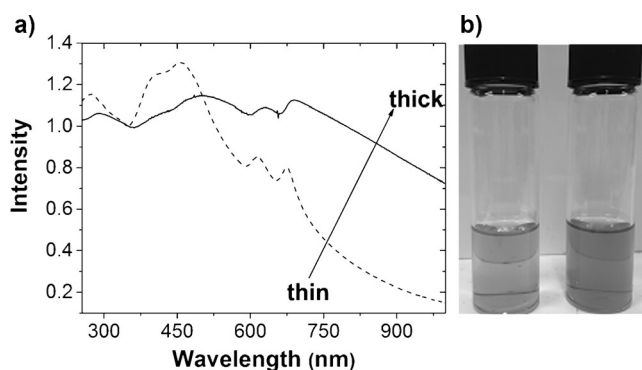


**Figure 1.** a) UV/Vis extinction spectra of 2H-MoS<sub>2</sub> (dashed trace) and Cys-2H-MoS<sub>2</sub> (solid trace) in IPA normalized to the local minimum at  $\approx 350$  nm. b) Photograph of diluted dispersions of 2H-MoS<sub>2</sub> (left) and Cys-2H-MoS<sub>2</sub> (right) in IPA.

in the Cys-2H-MoS<sub>2</sub>. Importantly, the DRIFT spectrum for Cys-2H-MoS<sub>2</sub> showed a number of new features that we attributed to the introduction of a cysteine derivative to the surface of the nanomaterial. A comparison of the DRIFT spectra of cysteine with Cys-2H-MoS<sub>2</sub> showed that the vibrational properties of the cysteine on the 2H-MoS<sub>2</sub> surface have been altered considerably through reaction with 2H-MoS<sub>2</sub>. Firstly, in cysteine a feature at  $2532 \text{ cm}^{-1}$  attributed to the  $\nu_{\text{S-H}}$  was observed.<sup>[41]</sup> This feature was absent in Cys-2H-MoS<sub>2</sub>, and there were no new features in this region of the DRIFT spectrum. This would suggest that the thiol group of cysteine had reacted in the presence of 2H-MoS<sub>2</sub>. All previous reports on the reaction between organic thiols and MoS<sub>2</sub> showed a similar loss of the  $\nu_{\text{S-H}}$  by IR spectroscopy, leading to the conclusion that the thiol had reacted with the MoS<sub>2</sub>.<sup>[27–35]</sup> Secondly, cysteine displayed broad features at  $1745$  and  $1377 \text{ cm}^{-1}$  corresponding to stretches of its carbox-

ylate group.<sup>[41]</sup> In Cys-2H-MoS<sub>2</sub> these features had shifted to lower energy (1644 and 1354 cm<sup>-1</sup>, respectively), presumably, again, as a result of a reaction between cysteine and 2H-MoS<sub>2</sub>. In all, the DRIFT spectrum of Cys-2H-MoS<sub>2</sub> indicated that cysteine is coupled to the surface of the 2H-MoS<sub>2</sub>. However, the clear and dramatic changes to the vibrational properties of the cysteine suggest that the cysteine had been chemically altered.

Raman spectroscopy also indicated that the reaction between cysteine and 2H-MoS<sub>2</sub> yielded a slightly altered 2H-MoS<sub>2</sub> surface. Minor changes to the relative intensities of resonantly enhanced features in the Raman spectrum (Supporting Information, Figures S1, S2) of Cys-2H-MoS<sub>2</sub> indicated organic functionalities were interacting with the 2H-MoS<sub>2</sub> surface.<sup>[36, 38, 42, 43]</sup>

To examine the atomic-level 2H-MoS<sub>2</sub>/cysteine interaction in Cys-2H-MoS<sub>2</sub>, high-resolution X-ray photoelectron spectroscopy (XPS) analysis was performed. First, we observed that the Cys-2H-MoS<sub>2</sub> nanosheets preserved the semiconducting 2H polymorph after functionalization, and were not the 1T polymorph.<sup>[23, 26, 44]</sup> The XPS spectrum of cysteine (Figure 3b) exhibited a single doublet of S 2p peaks

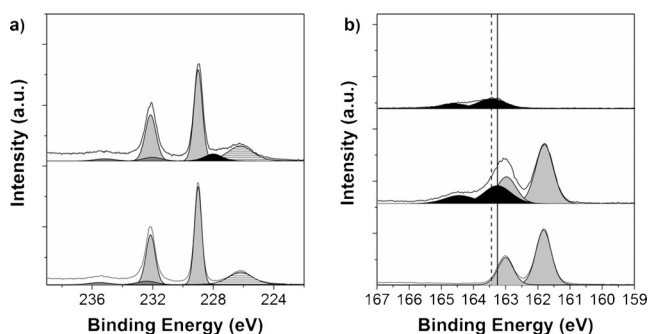


**Figure 3.** Fitted XPS spectra. a) Mo 3d core level spectra of Cys-2H-MoS<sub>2</sub> (top), and pristine 2H-MoS<sub>2</sub> (bottom). Fit components are attributed to 2H-MoS<sub>2</sub>, MoO<sub>3</sub>, S 2 s, and cysteine-like entities in both cases. b) S 2p core level spectra of cysteine salt (top), Cys-2H-MoS<sub>2</sub> (middle), and pristine 2H-MoS<sub>2</sub> (bottom). Fit components are attributed to 2H-MoS<sub>2</sub> (light gray), and cysteine-like entities (black).

with the S 2p<sub>3/2</sub> binding energy at 163.5 eV. In contrast, peak fitting of the S 2p spectrum of Cys-2H-MoS<sub>2</sub> resulted in two doublets. The first doublet with S 2p<sub>3/2</sub> binding energy at 161.8 eV made the largest contribution (68%) and was comparable to the S 2p<sub>3/2</sub> peak of the pristine 2H-MoS<sub>2</sub>. The smaller doublet with S 2p<sub>3/2</sub> binding energy at 163.3 eV was attributed to the surface cysteine entities. A minor shift (0.2 eV) in the binding energy in this doublet relative to pure cysteine was observed, consistent with a chemical change to the cysteine molecule. The higher binding energy component represented 32% of the S-atoms on the sample surface, indicating a degree of functionalization of 32%. We note that thermo-gravimetric analysis (TGA, below) also suggested ≈ 30% loading of cysteine in Cys-2H-MoS<sub>2</sub>.

Critically, the binding energy of the surface S-atoms in 2H-MoS<sub>2</sub> was not affected by the presence of a functional group on the nanosheet surface.<sup>[45]</sup> The S 2p XPS data was

best fit with only two S-atom components: a cysteine-like component and a 2H-MoS<sub>2</sub> component. Furthermore, the Mo 3d XPS spectra displayed no differences between 2H-MoS<sub>2</sub> and Cys-2H-MoS<sub>2</sub>, showing that the electronic environment around the Mo-atoms in Cys-2H-MoS<sub>2</sub> had not been altered upon functionalization. Previous reports showed that changes in the S 2p region of the XPS spectra of functionalized ce-1T-MoS<sub>2</sub> were indicative of the presence of functionality C- to MoS<sub>2</sub> S-bonds on the ce-1T-MoS<sub>2</sub> surface.<sup>[23, 26]</sup> These observations suggest that chemical modification of the 2H-MoS<sub>2</sub> surface in Cys-2H-MoS<sub>2</sub> was unlikely to have occurred, while a chemical modification of cysteine had occurred.

TGA of Cys-2H-MoS<sub>2</sub> revealed a clear stepwise degradation (Figure S3). Pristine 2H-MoS<sub>2</sub> did not display any degradation below 500 °C. In Cys-2H-MoS<sub>2</sub>, an approximately 30% weight loss took place between 215–265 °C. Because the thermal decomposition temperature of cysteine is 200–230 °C (Figure S3), we inferred that the significant weight loss was caused by the decomposition of cysteine-like molecules bound to the 2H-MoS<sub>2</sub> surface. According to TGA-coupled infra-red (TGA-IR) spectroscopy, the major gaseous product evolved from Cys-2H-MoS<sub>2</sub> was identified as CO<sub>2</sub> (Figure S4, 2349 cm<sup>-1</sup>) which presumably derives from the decomposition of cysteine. The TGA thus indicated that an organic functionality, very similar to cysteine, was docked on 2H-MoS<sub>2</sub> in Cys-2H-MoS<sub>2</sub>.

Having thoroughly characterized Cys-2H-MoS<sub>2</sub>, we then probed the effect of the cysteine functionalities on the dispersability of the 2H-MoS<sub>2</sub>. We found that Cys-2H-MoS<sub>2</sub> was readily re-dispersed in water (Figure S6). Pristine 2H-MoS<sub>2</sub> did not disperse in water (Figure S6), and few methods to effectively disperse 2H-MoS<sub>2</sub> in water by functionalization exist.<sup>[30, 46]</sup> Importantly, the aqueous Cys-2H-MoS<sub>2</sub> dispersions were stable for at least one week. Furthermore, we could vary the pH of the aqueous dispersions, with no effect on the dispersability of the Cys-2H-MoS<sub>2</sub> (Figure S6). We previously identified methods to enhance TMD dispersability in acetone,<sup>[25]</sup> but the present water dispersion results are very important, potentially eliminating the use of organic solvents altogether for 2H-MoS<sub>2</sub>.

We performed a number of experiments to verify the nature of the interaction between 2H-MoS<sub>2</sub> and cysteine. As stated earlier, XPS indicated that no change to the MoS<sub>2</sub> S- or Mo-atoms in Cys-2H-MoS<sub>2</sub> had occurred, with a very minor change to the surface cysteine. These observations indicated that the functionalization in Cys-2H-MoS<sub>2</sub> may not be covalent, and also suggested that cysteine S-atoms may not be filling S-atom vacancies. However, the surface properties of the 2H-MoS<sub>2</sub> in Cys-2H-MoS<sub>2</sub> had clearly been altered, as evidenced by UV/Vis spectroscopy and re-dispersion measurements. XPS, TGA, and Raman analyses confirmed the presence of surface functionalities in Cys-2H-MoS<sub>2</sub>. However, these analyses provided no evidence for covalent or dative bond formation between the 2H-MoS<sub>2</sub> and functionality. Finally, the DRIFT measurements suggested a chemical change to the cysteine molecules on the surface, while the 2H-MoS<sub>2</sub> remained in a pristine state.

To probe the surface functional groups further, we removed them from the surface (de-functionalization). De-



functionalization was achieved by first dispersing the Cys-2H-MoS<sub>2</sub> in IPA and subsequently centrifuging this dispersion and decanting the IPA. Second, after multiple such washings, the resultant solids were re-dispersed in water, placed in a dialysis bag, and dialyzed for four days. After dialysis, the solvent was removed from the resulting dialysate under vacuum, and the obtained product (de-functionalized organic material) was analyzed by <sup>1</sup>H NMR, while the resulting 2H-MoS<sub>2</sub> was subjected to XPS. The <sup>1</sup>H NMR spectrum (Figure S8) of the dialysate product showed that the obtained material was not cysteine, but in fact was the oxidized (disulfide) derivative of cysteine, cystine. The identification of the disulfide product accounts for the disappearance of the ν<sub>S-H</sub> resonance in the DRIFT spectrum of Cys-2H-MoS<sub>2</sub>. XPS analysis of the post-dialysis 2H-MoS<sub>2</sub> showed that the de-functionalized nanomaterial was pristine 2H-MoS<sub>2</sub> (Figure S9, no organic S-features, confirming complete de-functionalization). Critically, when 2H-MoS<sub>2</sub> was reacted with cystine, we observed the same DRIFT and XPS features in the resulting functionalized material as we observed for Cys-2H-MoS<sub>2</sub> (Figure S17,18), showing physisorption of cystine on 2H-MoS<sub>2</sub>. These observations demonstrate that the reaction between cysteine and 2H-MoS<sub>2</sub> caused the thiol to be converted to a new entity, but the 2H-MoS<sub>2</sub> was chemically unchanged.

We then compared the DRIFT spectrum of Cys-2H-MoS<sub>2</sub> with the DRIFT spectrum of cystine (Figure 4). The spectra showed an almost perfect overlap of resonances (of particular note is the S–S vibrational mode, ν<sub>S-S</sub> = 540 cm<sup>-1</sup>),<sup>[47]</sup> demonstrating that cystine (and not cysteine) was docked on the

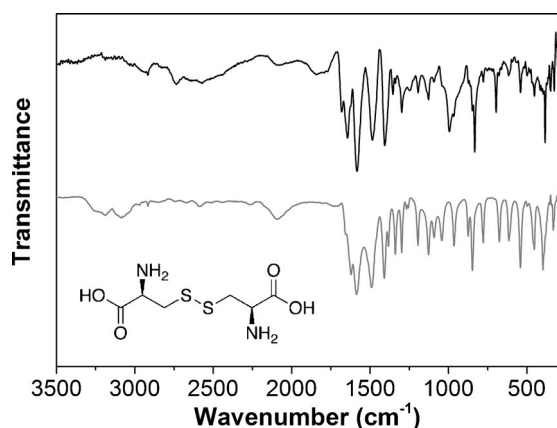


**Figure 4.** DRIFT spectra of Cys-2H-MoS<sub>2</sub> (black trace) and cystine (gray trace).

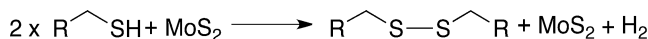
surface in Cys-2H-MoS<sub>2</sub>. The lack of a chemical change to the 2H-MoS<sub>2</sub> in Cys-2H-MoS<sub>2</sub>, and ease at which the cystine was de-functionalized from the surface, would suggest that cystine was simply physisorbed onto the 2H-MoS<sub>2</sub> surface. This is an important observation and probably accounts for the very high degree of loading of organic functionalities (Figure S5). Only through physisorption of multiple layers of organic functionality would such high levels of loading be achievable.

We were intrigued by the 2H-MoS<sub>2</sub> facilitated oxidation of cysteine to cystine yielding functionalization through

physisorption of cystine. Earlier work demonstrated the functionalization of ce-1T-MoS<sub>2</sub> through ligand conjugation.<sup>[26]</sup> We explored the reaction of cysteine with ce-1T-MoS<sub>2</sub> (following the ligand conjugation methods) and obtained DRIFT and XPS spectra that showed cystine was docked onto the surface of ce-1T-MoS<sub>2</sub> (Figures S10 and S11), rather than cysteine. Thus, in both 2H- and 1T-polymorphs of MoS<sub>2</sub>, their reaction with cysteine yielded cystine-functionalized MoS<sub>2</sub>. We then performed the reaction between cysteine and 2H-MoS<sub>2</sub> under an inert atmosphere (N<sub>2</sub>). Under these conditions, we obtained the same Cys-2H-MoS<sub>2</sub>, containing the disulfide product cystine, as evidenced by DRIFT spectroscopy (Figure S12). This demonstrated that dioxygen was not facilitating the oxidation of cysteine to cystine, and that MoS<sub>2</sub> is likely the mediator of this transformation. To explore if oxidation was caused by the functionalization methods, we sonicated a solution of cysteine in IPA in the absence of MoS<sub>2</sub> (thus under the functionalization conditions). The <sup>1</sup>H-NMR spectrum (Figure S13) of the solids resulting from this experiment showed resonances typical of cysteine, and not cystine, verifying that the functionalization methods do not lead to the oxidation of cysteine. Finally, the analogous reaction between cysteine and liquid exfoliated 2H-WS<sub>2</sub> yielded similar results to 2H-MoS<sub>2</sub> (thus Cys-2H-WS<sub>2</sub>, with cystine functionalities; Figure S16).

We also attempted the functionalization of liquid-exfoliated 2H-MoS<sub>2</sub> with other commercially available thiols (1-octanethiol, 3-mercaptopropionic acid) and identified oxidized disulfide products. The DRIFT spectrum of the products showed characteristic S–S vibrational features, suggesting the formation of disulfides (Figures S14, S15). The observation of ν<sub>C-S</sub> = 615 cm<sup>-1</sup>, as observed previously for dioctyl-disulfide-functionalized nanoparticles,<sup>[48]</sup> provided a very strong indication of disulfide formation when 1-octanethiol reacted with 2H-MoS<sub>2</sub>. Furthermore, GC-MS analysis of the 2H-MoS<sub>2</sub>/thiol reaction mixtures showed the presence of disulfide products (Figures S14, S15). It thus appears that TMDs facilitate the oxidation of organic thiols to disulfides. The formed disulfides appear to have physisorbed on the 2D TMD surface, presumably through electrostatic interactions.

The mechanism of disulfide formation is, at the moment, not clear to us. Because the oxidation of disulfides does not require O<sub>2</sub>, we therefore propose that that MoS<sub>2</sub> is mediating the conversion of thiols to disulfide with the concomitant release of H<sub>2</sub> (Scheme 2). We think thiols donate a hydrogen



**Scheme 2.** MoS<sub>2</sub>-mediated conversion of organic thiol to disulfide.

atom to MoS<sub>2</sub>, yielding a thiyl radical and a 1-electron-reduced product H[MoS<sub>2</sub>]. The thiyl radical presumably reacts with another thiyl radical to yield disulfide. The H[MoS<sub>2</sub>] possibly releases dihydrogen through the coupling of two H-atoms bound to the polymeric MoS<sub>2</sub> surface. This hypothesis requires extensive study to confirm the mechanism.

In conclusion, we have demonstrated a general route for the functionalization of 2H-MoS<sub>2</sub> nanosheets with cysteine. Functionalization was achieved by blending a dispersion of liquid-exfoliated 2H-MoS<sub>2</sub> with a solution of cysteine. The resulting Cys-2H-MoS<sub>2</sub> was fully characterized by UV/Vis, DRIFT, XPS, TGA, and Raman spectroscopy. We discovered that MoS<sub>2</sub> was facilitating the oxidation of cysteine to cystine during functionalization. Rather than coordinating as a thiol (cysteine) at S-vacancies in the 2H-MoS<sub>2</sub>, as originally conceived, cystine was simply physisorbed on the nanosheet. These observations were found to be true for other organic thiols, and indeed other TMDs. Based on our findings, we urge caution with methods that employ organic thiols to chemically functionalize TMDs; the thiols may not be forming bonds with the surface. Present explorations in our lab are focused on alternative methods for the covalent functionalization of 2H-MoS<sub>2</sub>.

## Acknowledgements

This publication has emanated from research supported in part by the European Union (FP7-333948, AMcD) and a research grant from Science Foundation Ireland (SFI/12/RC/2278). CB acknowledges the German research foundation DFG (BA 4856/1-1). GSD acknowledges SFI (PI<sub>10</sub>/IN.1/I3030).

**Keywords:** 2D materials · liquid exfoliation · organic thiol · surface functionalization · transition metal dichalcogenides

**How to cite:** *Angew. Chem. Int. Ed.* **2016**, *55*, 5803–5808  
*Angew. Chem.* **2016**, *128*, 5897–5902

- [1] H. Zhang, K. P. Loh, C. H. Sow, H. Gu, X. Su, C. Huang, Z. K. Chen, *Langmuir* **2004**, *20*, 6914–6920.
- [2] B. Radisavljevic, A. Radenovic, J. Brivio, V. Giacometti, A. Kis, *Nat. Nanotechnol.* **2011**, *6*, 147–150.
- [3] G. Eda, H. Yamaguchi, D. Voiry, T. Fujita, M. Chen, M. Chhowalla, *Nano Lett.* **2011**, *11*, 5111–5116.
- [4] Y. Li, H. Wang, L. Xie, Y. Liang, G. Hong, H. Dai, *J. Am. Chem. Soc.* **2011**, *133*, 7296–7299.
- [5] K.-K. Liu, W. Zhang, Y.-H. Lee, Y.-C. Lin, M.-T. Chang, C.-Y. Su, C.-S. Chang, H. Li, Y. Shi, H. Zhang, C.-S. Lai, L.-J. Li, *Nano Lett.* **2012**, *12*, 1538–1544.
- [6] T. Cao, G. Wang, W. Han, H. Ye, C. Zhu, J. Shi, Q. Niu, P. Tan, E. Wang, B. Liu, J. Feng, *Nat. Commun.* **2012**, *3*, 887.
- [7] K. F. Mak, K. He, J. Shan, T. F. Heinz, *Nat. Nanotechnol.* **2012**, *7*, 494–498.
- [8] H. Zeng, J. Dai, W. Yao, D. Xiao, X. Cui, *Nat. Nanotechnol.* **2012**, *7*, 490–493.
- [9] H. J. Conley, B. Wang, J. I. Ziegler, R. F. Haglund, S. T. Pantelides, K. I. Bolotin, *Nano Lett.* **2013**, *13*, 3626–3630.
- [10] K. Lee, R. Gatensby, N. McEvoy, T. Hallam, G. S. Duesberg, *Adv. Mater.* **2013**, *25*, 6699–6702.
- [11] V. Nicolosi, M. Chhowalla, M. G. Kanatzidis, M. S. Strano, J. N. Coleman, *Science* **2013**, *340*, 1420.
- [12] X. Chen, A. R. McDonald, *Adv. Mater.* **2016**, DOI: 10.1002/adma.201505345.
- [13] Q. H. Wang, K. Kalantar-Zadeh, A. Kis, J. N. Coleman, M. S. Strano, *Nat. Nanotechnol.* **2012**, *7*, 699–712.
- [14] M. Chhowalla, H. S. Shin, G. Eda, L.-J. Li, K. P. Loh, H. Zhang, *Nat. Chem.* **2013**, *5*, 263–275.
- [15] J. N. Coleman, M. Lotya, A. O'Neill, S. D. Bergin, P. J. King, U. Khan, K. Young, A. Gaucher, S. De, R. J. Smith, I. V. Shvets, S. K. Arora, G. Stanton, H.-Y. Kim, K. Lee, G. T. Kim, G. S. Duesberg, T. Hallam, J. J. Boland, J. J. Wang, J. F. Donegan, J. C. Grunlan, G. Moriarty, A. Shmeliov, R. J. Nicholls, J. M. Perkins, E. M. Grieveson, K. Theuvsen, D. W. McComb, P. D. Nellist, V. Nicolosi, *Science* **2011**, *331*, 568–571.
- [16] H. Li, Z. Yin, Q. He, H. Li, X. Huang, G. Lu, D. W. H. Fam, A. I. Y. Tok, Q. Zhang, H. Zhang, *Small* **2012**, *8*, 63–67.
- [17] Y. Zhan, Z. Liu, S. Najmaei, P. M. Ajayan, J. Lou, *Small* **2012**, *8*, 966–971.
- [18] M. O'Brien, N. McEvoy, T. Hallam, H.-Y. Kim, N. C. Berner, D. Hanlon, K. Lee, J. N. Coleman, G. S. Duesberg, *Sci. Rep.* **2014**, *4*, 7374.
- [19] C. Yim, M. O'Brien, N. McEvoy, S. Riazimehr, H. Schäfer-Eberwein, A. Bablich, R. Pawar, G. Iannaccone, C. Downing, G. Fiori, M. C. Lemme, G. S. Duesberg, *Sci. Rep.* **2014**, *4*, 5458.
- [20] Z. Zeng, Z. Yin, X. Huang, H. Li, Q. He, G. Lu, F. Boey, H. Zhang, *Angew. Chem. Int. Ed.* **2011**, *50*, 11093–11097; *Angew. Chem.* **2011**, *123*, 11289–11293.
- [21] A. Splendiani, L. Sun, Y. Zhang, T. Li, J. Kim, C.-Y. Chim, G. Galli, F. Wang, *Nano Lett.* **2010**, *10*, 1271–1275.
- [22] K. F. Mak, C. Lee, J. Hone, J. Shan, T. F. Heinz, *Phys. Rev. Lett.* **2010**, *105*, 136805.
- [23] K. C. Knirsch, N. C. Berner, H. C. Nerl, C. S. Cucinotta, Z. Gholamvand, N. McEvoy, Z. Wang, I. Abramovic, P. Vecera, M. Halik, S. Sanvito, G. S. Duesberg, V. Nicolosi, F. Hauke, A. Hirsch, J. N. Coleman, C. Backes, *ACS Nano* **2015**, *9*, 6018–6030.
- [24] D. Voiry, A. Goswami, R. Kappera, C. de Carvalho Castro e Silva, D. Kaplan, T. Fujita, M. Chen, T. Asefa, M. Chhowalla, *Nat. Chem.* **2015**, *7*, 45–49.
- [25] C. Backes, N. C. Berner, X. Chen, P. Lafargue, P. LaPlace, M. Freeley, G. S. Duesberg, J. N. Coleman, A. R. McDonald, *Angew. Chem. Int. Ed.* **2015**, *54*, 2638–2642; *Angew. Chem.* **2015**, *127*, 2676–2680.
- [26] S. S. Chou, M. De, J. Kim, S. Byun, C. Dykstra, J. Yu, J. Huang, V. P. Dravid, *J. Am. Chem. Soc.* **2013**, *135*, 4584–4587.
- [27] M. Makarova, Y. Okawa, M. Aono, *J. Phys. Chem. C* **2012**, *116*, 22411–22416.
- [28] S.-D. Jiang, G. Tang, Z.-M. Bai, Y.-Y. Wang, Y. Hu, L. Song, *RSC Adv.* **2014**, *4*, 3253–3262.
- [29] L. Zhou, B. He, Y. Yang, Y. He, *RSC Adv.* **2014**, *4*, 32570–32578.
- [30] R. Anbazhagan, H.-J. Wang, H.-C. Tsai, R.-J. Jeng, *RSC Adv.* **2014**, *4*, 42936–42941.
- [31] J.-S. Kim, H.-W. Yoo, H. O. Choi, H.-T. Jung, *Nano Lett.* **2014**, *14*, 5941–5947.
- [32] Z. Yu, Y. Pan, Y. Shen, Z. Wang, Z.-Y. Ong, T. Xu, R. Xin, L. Pan, B. Wang, L. Sun, J. Wang, G. Zhang, Y. W. Zhang, Y. Shi, X. Wang, *Nat. Commun.* **2014**, *5*, 5290.
- [33] T. Liu, S. Shi, C. Liang, S. Shen, L. Cheng, C. Wang, X. Song, S. Goel, T. E. Barnhart, W. Cai, Z. Liu, *ACS Nano* **2015**, *9*, 950–960.
- [34] E. P. Nguyen, B. J. Carey, J. Z. Ou, J. van Embden, E. D. Gaspera, A. F. Chrimes, M. J. S. Spencer, S. Zhuiykov, K. Kalantar-zadeh, T. Daeneke, *Adv. Mater.* **2015**, *27*, 6224–6229.
- [35] K. Cho, M. Min, T.-Y. Kim, H. Jeong, J. Pak, J.-K. Kim, J. Jang, S. J. Yun, Y. H. Lee, W.-K. Hong, T. Lee, *ACS Nano* **2015**, *9*, 8044–8053.
- [36] M. Donarelli, F. Bisti, F. Perrozzi, L. Ottaviano, *Chem. Phys. Lett.* **2013**, *588*, 198–202.
- [37] H. Qiu, T. Xu, Z. Wang, W. Ren, H. Nan, Z. Ni, Q. Chen, S. Yuan, F. Miao, F. Song, G. Long, Y. Shi, L. Sun, J. Wang, X. Wang, *Nat. Commun.* **2013**, *4*, 2642.
- [38] H.-P. Komsa, S. Kurasch, O. Lehtinen, U. Kaiser, A. V. Krashe-ninnikov, *Phys. Rev. B* **2013**, *88*, 035301.
- [39] C. Backes, R. J. Smith, N. McEvoy, N. C. Berner, D. McCloskey, H. C. Nerl, A. O'Neill, P. J. King, T. Higgins, D. Hanlon, N.

- Scheuschner, J. Maultzsch, L. Houben, G. S. Duesberg, J. F. Donegan, V. Nicolosi, J. N. Coleman, *Nat. Commun.* **2014**, *5*, 4576.
- [40] G. Berhault, L. Cota Araiza, A. Duarte Moller, A. Mehta, R. Chianelli, *Catal. Lett.* **2002**, *78*, 81–90.
- [41] A. Pawlukojć, J. Leciejewicz, A. J. Ramirez-Cuesta, J. Nowicka-Scheibe, *Spectrochim. Acta Part A* **2005**, *61*, 2474–2481.
- [42] X. Zhang, X.-F. Qiao, W. Shi, J.-B. Wu, D.-S. Jiang, P.-H. Tan, *Chem. Soc. Rev.* **2015**, *44*, 2757–2785.
- [43] M. A. Pimenta, E. del Corro, B. R. Carvalho, C. Fantini, L. M. Malard, *Acc. Chem. Res.* **2015**, *48*, 41–47.
- [44] This is evident in features in the Mo 3d core level spectra identified at 229.0 and 232.1 eV for Mo 3d<sub>5/2</sub> and Mo 3d<sub>3/2</sub> respectively (Figure 3a). If it were 1T-MoS<sub>2</sub>, features at 228.6 and 231.7 ± 0.15 eV would be expected, supporting our UV/Vis observations.
- [45] A mild broadening of the S 2p component attributed to 2H-MoS<sub>2</sub> (161.8 eV) is not significant enough to suggest chemical modification.
- [46] W. Zhang, Y. Wang, D. Zhang, S. Yu, W. Zhu, J. Wang, F. Zheng, S. Wang, J. Wang, *Nanoscale* **2015**, *7*, 10210–10217.
- [47] E. J. Bastian, R. B. Martin, *J. Phys. Chem.* **1973**, *77*, 1129–1133.
- [48] B. S. Zelakiewicz, G. C. Lica, M. L. Deacon, Y. Y. Tong, *J. Am. Chem. Soc.* **2004**, *126*, 10053–10058.

Received: November 3, 2015

Revised: December 23, 2015

Published online: April 1, 2016